GEOPHYSICAL RESEARCH LETTERS, VOL. 28, NO. 20, PAGES 3999-4002, OCTOBER 15, 2001

Tidal triggering of microearthquakes on the Juan de Fuca Ridge

William S. D. Wilcock

School of Oceanography, University of Seattle, Seattle

Abstract. Tidal stresses beneath the oceans can be up to an order of magnitude higher than those found in the continents because of the effects of loading by ocean tides. I have analyzed 1899 microearthquakes recorded during a 55-day experiment on the Endeavour segment of the Juan de Fuca Ridge for tidal triggering. The tidal phase of the full data set and of a declustered subset comprising 987 events appears non-random to a high level of confidence. Earthquakes occur more frequently near low tides, especially the lowest spring tides, when the extensional stresses are a maximum in all directions.

Introduction

Tidal stress variations [*Melchior*, 1983] are orders of magnitude smaller than the typical stress drops that accompany earthquakes [*Kanamori and Anderson*, 1975], but in most settings the rates of stress change due to tides are significantly higher than average rates of tectonic stress buildup. If earthquakes were triggered immediately at a threshold stress, they should occur more frequently near tidal extremes. Although the conclusions of tidal triggering studies are varied [*Emter*, 1997], it is clear that there is not a universally strong correlation between earthquakes and tides

The simplest explanation for a lack of tidal triggering is that earthquakes are preceded by an interval of accelerating stress buildup or fault weakening [*Vidale et al.*, 1998; *Lockner and Beeler*, 1999]. Quantifying weak correlations, or the lack thereof, can constrain the processes that lead to earthquake nucleation. In a recent study of over 13,000 California earthquakes, *Vidale et al.* [1998] find that the rate of earthquakes is 2% higher when the stress favors rupture but that the difference is not statistically significant at the 95% confidence level. They conclude that preseismic stress rates in earthquake nucleation zones are at least 15 kPa/hr, far in excess of the long-term tectonic stress rate of 10 Pa/hr.

The oceans may be a good environment to search for tidal triggering because ocean loading increases tidal stresses [*Emter*, 1997]. In the continents, solid earth tidal stresses have amplitudes of 1-4 kPa [*Melchior*, 1983]. In the oceans, tidal ranges can reach several meters (1 m = 10 kPa). In this paper, I present an analysis of earthquakes recorded by a local network on a mid-ocean ridge that reveals evidence for tidal triggering.

Paper number 2001GL013370.
0094-8276/01/2001GL013370$05.00

Microearthquake data set

The data set used in this study was collected in the summer of 1995 on the Endeavour segment of the Juan de Fuca Ridge. The experiment (Figure 1) is described in detail by *Wilcock et al.* [2001]. Fifteen ocean bottom seismometers (OBSs) were deployed near the center of the segment for 55 days. The network spanned a 5-km section of the ridge axis that enclosed two hydrothermal vent fields and extended 15 km off-axis to the west. High levels of seismicity were recorded throughout the experiment both on- and off-axis. A total of 1899 earthquakes were located with at least 4 arrival times. Seismic moments range from 10^9 to 4×10^{13} N m. There are 1498 earthquakes within 5 km of the nearest OBS of which 746 are located in a band of axial seismicity at 1.5-3.5 km depth beneath the vent fields. Focal mechanisms for the better recorded axial earthquakes are quite variable and are characterized by subhorizontal tension axes. On the west flank, the earthquakes occur primarily in swarms, many of which are to the north of the network. Well-constrained focal depths are mostly between 2 and 4.5 km. Focal mechanisms show ridge parallel extension and north-south compression. Several large swarms are also located well outside the network on the east flank and near the ridge axis to the north and south of the network.

Evidence for tidal triggering

The Northeast Pacific Ocean has large tides [*Mofjeld et al.*, 1995]. The experiment coincided with maximum summer tidal ranges that twice exceeded 3.5 m (Figure 2a). A histogram of the earthquake count (Figure 2b) appears to show increased levels of seismicity during intervals with large tidal ranges and more earthquakes near or just after the lowest tides.

In order to search quantitatively for tidal triggering, I first estimated the tidal perturbations to crustal stresses. Horizontal tidal strains at the seafloor were obtained by summing the contributions from solid earth tides [*Berger*, 1969] and ocean-tide loading [*Agnew*, 1997] assuming the tidal model of *Schwiderski* [1980]. Tidal perturbations to the vertical principal stress at the seafloor were obtained directly from predicted variations in seafloor pressure [*Mofjeld et al.*, 1995]. By assuming that the perturbations to vertical stress and horizontal strain are invariant with depth, I estimated the tidal stress tensor at mid-crustal depths (Figure 2c) using elastic constants consistent with $V_P = 6.5$ km/s, $V_S = 3.5$ km/s, and a density of 2800 kg/m^3.

If the fault planes and slip directions are known, it is possible to resolve the tidal stress perturbations on each fault. For the Endeavour data set, focal mechanisms are available for 173 earthquakes [*Wilcock et al.*, 2001]. However, with the exception of a few swarms that were relocated using a

cross-correlation technique, the fault plane ambiguity is unresolved. Thus, this study was limited to looking at the correlation between earthquakes and the tidal stresses at fixed orientations.

A common method to search for tidal triggering is to calculate the tidal phase of origin times and use statistical methods to determine whether earthquakes are randomly distributed within the semidiurnal tidal cycle [*Emter*, 1997]. At the Endeavour site the tidal stress components (Figure 2b) are roughly in phase and the rose plots of tidal phase distributions (Figure 3) are similar for a variety of parameters. The earthquake frequency is lowest at high tide and highest at low tide and in the quadrant following low tide (Figure 3a). Low tide corresponds to a maximum in cubic stress (the trace of the stress tensor) when the tensional normal stress is a maximum in all directions (Figure 3b). The highest earthquake frequencies are observed when the extensional stress perpendicular to the ridge axis is near a maximum (Figure 3c) but when the shear stress driving normal faulting on ridge-parallel faults dipping at 45°is near a minimum (Figure 3d).

The probability P_R that the phase distribution is random can be approximated:

$$P_R = exp\left(\frac{-R^2}{N}\right) \quad (1)$$

where R is the length of the vector sum of the phasors and N the number of earthquakes [*Emter*, 1997]. This is commonly termed a Schuster test. For these data (Figure 3), it shows that the probability of achieving the observed distributions by a random process is extremely low ($\leq \ 1 \times 10^{-9}$). Is this result robust? One of the characteristics of the Schuster test is that a small number of nonrandom events within a sequence can lead to a positive test [*Rydelek et al.*, 1992].

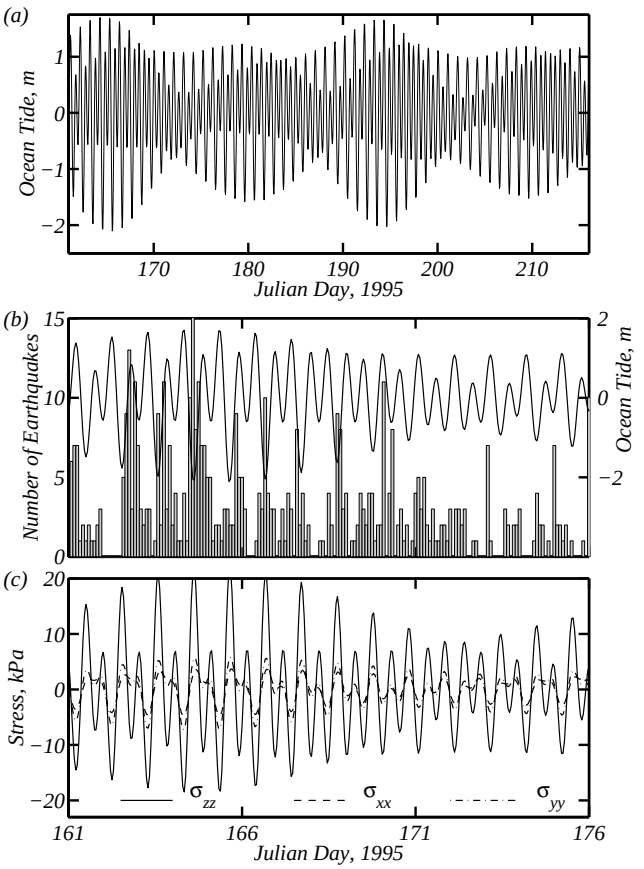

Figure 2. (a) Time series of predicted ocean tides during the experiment at 48°N, 129°W *Mofjeld et al.* [1995]. (b) Fifteen-day time histogram of the earthquake count in 2 hour bins with the ocean tide time series superimposed. (c) Estimates of mid-crustal normal stresses in vertical (solid), E-W (dashed) and N-S (dot-dashed) directions. Extensional stresses are positive.

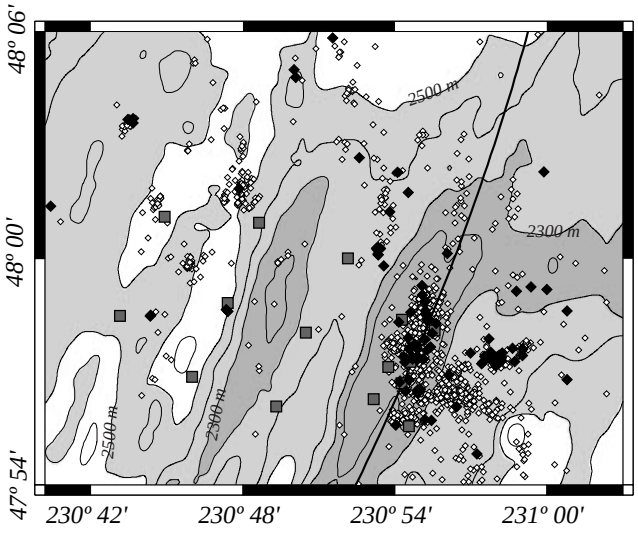

Figure 1. Smoothed bathymetric map of the central portion of the Endeavour segment with the ridge axis marked by a solid line, showing the location of the ocean bottom seismometers (gray squares) and epicenters (open and filled diamonds) for the microearthquake experiment *Wilcock et al.* [2001]. Filled diamonds indicate earthquakes that occurred during the lowest tides (<-1.5 m) when the rate of seismicity approached twice the average for the experiment.

The noise levels on the seafloor recorders do not vary systematically with the tides or time of day so the correlation is not a result of variations in detection threshold.

A weakness of my analysis is that many of the earthquakes occurred in swarms [*Wilcock et al.*, 2001]; the tidal phases of individual earthquakes within a swarm are not fully independent. If a Schuster test is used to search for periodicity between 1 hour and 2 days, a nonrandom distribution at 95% significance is found for 60% of the periods. To minimize the influence of swarms, I used an algorithm [*Reasenberg*, 1985] to remove all but the first event in spatially and temporarily clustered sequences. The phase distributions of the 987 earthquakes in the declustered catalog are also shown in Figure 3. The values of P_R are larger than for the whole data set as would be expected for a smaller sample, but the distributions are still nonrandom to a high level of confidence.

I also investigated the frequency of earthquakes as a function of tide height and tidal stress (Figure 4). The earthquake frequency nearly doubles at the lowest tides (these correspond to a six-monthly minimum) and at the highest cubic and extensional stresses. The trends are similar for the declustered earthquakes and appear quite robust. If the declustered earthquakes were distributed uniformly through the experiment, 36 would occur when the tide is below -1.5

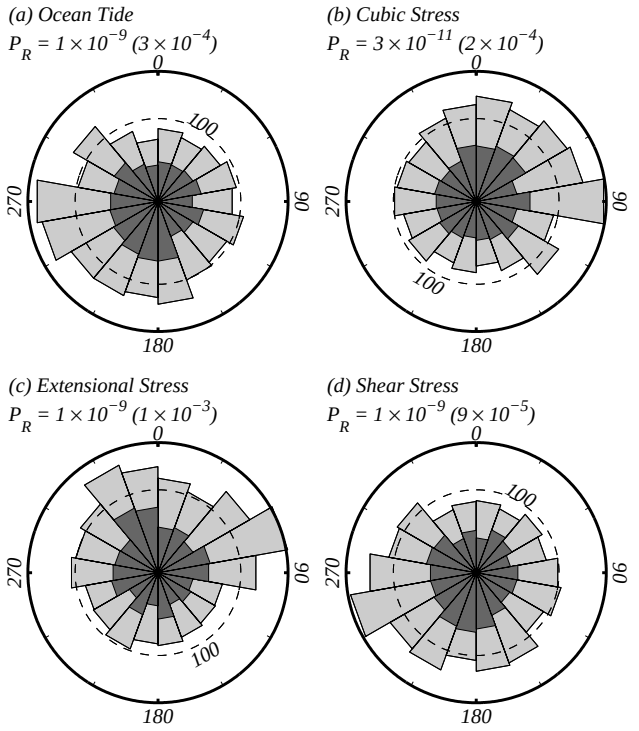

Figure 3. Rose diagrams showing the distribution of earthquakes as a function of their phase within the semidiurnal cycle of (a) ocean tide height, (b) cubic stress, (c) the extensional stress perpendicular to the ridge axis and (d) the shear stress driving normal faulting on ridge-parallel faults dipping at 45°. Phases were calculated relative to successive tidal maxima. Results are shown for all earthquakes (light gray) and the declustered earthquakes (dark gray). The probability P_R that these distributions are the result of random processes is listed above each plot with the value for the declustered data set in parentheses.

m, but 59 were observed. The probability of observing at least this many in a random sequence is only 0.01%. The epicenters for events that occur at the lowest tides are distributed throughout the seismically active areas (Figure 1).

Discussion

Investigations that find evidence for tidal triggering are often controversial. It is difficult to prove weak correlations in complex data sets and many studies suffer from a lack of statistical rigor [*Emter*, 1997]. In this study, there is evidence for increased earthquake frequency during the lowest tides. The analysis would benefit from a longer observation period that spanned several six-monthly tidal minima and more information about fault orientations. It is also complicated by the presence of swarms, although the results are similar when these are excluded.

This study is not the first to find evidence for tidal triggering in oceanic regions. *Berg* [1966] reported that the 1964 Alaskan earthquake and most of its aftershocks occurred at low tide. A study of nearly 1000 globally distributed earthquakes [*Tsuruoka et al.*, 1995] finds a significant correlation for a subset of 75 normal faulting earthquakes located primarily on mid-ocean ridges. Microearthquakes recorded on Axial Seamount of the Juan de Fuca Ridge are also correlated with tides [*Tolstoy et al.*, 2001].

The phase relationships I observe are consistent with a tidal triggering mechanism. Low tide corresponds to the time when all three principal stresses are most extensional (Figure 2c). The extensional normal stress will be a maximum on all fault planes, while the sign of the resolved tidal shear stress will depend on the fault orientation. For a heterogeneous distribution of fault planes, the average Coulomb stress driving fault motions will generally be a maximum at low tides. Seismicity along most ridges is characterized by ridge-parallel normal faults, but focal mechanisms and relative relocations show that the fault orientations are more variable on the Endeavour segment [*Wilcock et al.*, 2001].

At the Endeavour site, tidal stresses are dominated by ocean loading and vertical stress variations can reach up to 30-40 kPa (Figure 1c), an order of magnitude higher than typical tidal stresses in the continents [*Melchior*, 1983]. Laboratory simulations [*Lockner and Beeler*, 1999] show that sequences of 20 stick-slip events at a confining pressure of 50 MPa are correlated with an imposed periodic loading function once the amplitude exceeds ∼100 kPa. Simple statistical arguments [*Lockner and Beeler*, 1999] suggest that ∼200 and ∼20,000 events would be required to resolve a correlation for perturbations of 30 and 3 kPa, respectively. This inference is consistent with this study and the analysis of Californian seismicity [*Vidale et al.*, 1998].

Studies of earthquakes triggered by surface waves in California [*Hill et al.*, 1993] and Greece [*Brodsky et al.*, 2000] show that seismicity is preferentially triggered in volcanic and geothermal regions that are often under extension, characteristics that are all applicable to mid-ocean ridges. Trig-

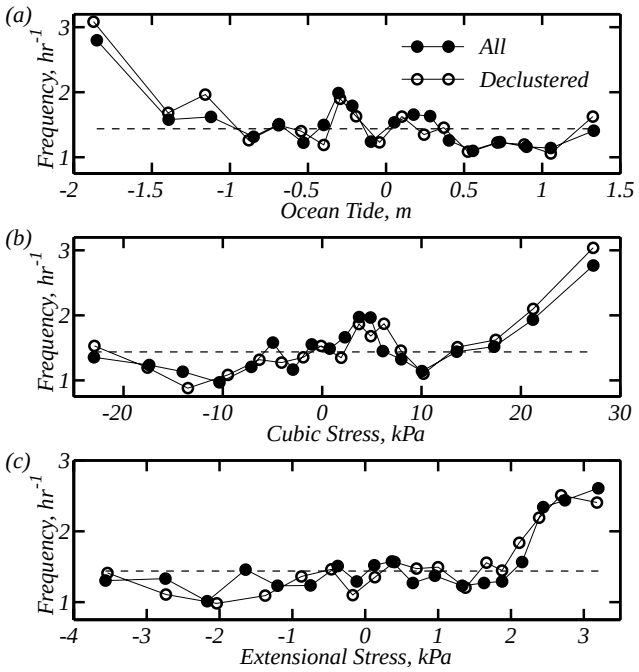

Figure 4. Frequency (number per hour) of located earthquakes plotted as a function of the predicted (a) ocean tide height, (b) cubic stress and (c) ridge-perpendicular extensional stress at the time of the earthquake. Plots are shown for all earthquakes (solid circles) and declustered earthquakes (open circles). Each point is based on ∼100 and ∼55 earthquakes for the full and declustered data sets, respectively. Dashed lines show the average earthquake frequency.

gering may be related to nonlinear interactions between strain fluctuations and hydrothermal or magmatic fluids [*Hill et al.*, 1993]. The threshold stress for dynamic triggering is generally 200-600 kPa [*Brodsky et al.*, 2000], much higher than the tidal stresses on the Endeavour segment. This difference might reflect a change in the triggering mechanism or differences in the perturbation period. The threshold may also be sensitive to the depth of seismicity; tidal perturbations will have a larger proportional effect at shallow depths. One explanation for a low trigger threshold (∼10 kPa) at The Geysers, California [*Gomberg and Davis*, 1996] is the shallow depth of seismicity [*Lockner and Beeler*, 1999].

Acknowledgments. I thank Mike Purdy for his many contributions to the experiment; John Bailey, Jim Dolan, David DuBois, John Hallinan, and Beecher Wooding for their expertise with the OBS instruments; the captain and crew of the *R/VWecoma* for their assistance at sea; Duncan Agnew, Hal Mofjeld and Paul Reasenberg for algorithms and helpful discussions; and two anonymous referees. This work was supported by the National Science Foundation under grant OCE-9403668.

References

Agnew, D., NLOADF: A program for computing ocean-tide loading, *J. Geophys. Res, 102, 5109-5110,* 1997.

Berg, E., Triggering of the Alaskan earthquake of March 28, 1964, and major aftershocks by low ocean tide loads, *Nature, 210,* 893-896, 1966.

Berger, J., A laser earth strain meter, Ph.D. thesis, University of California, San Diego, 1969.

Brodsky, E. E., V. Karakostas, and H. Kanamori, A new observation of dynamically triggered regional seismicity: Earthquakes in Greece following the August, 1999 Izmit, Turkey earthquake, *Geophys. Res. Lett., 27,* 2741-2744, 2000.

Emter, D., Tidal triggering of earthquakes and volcanic events, in *Tidal Phenomena,* edited by S. Bhattacharji, G. Friedman, H. J. Neugebauer, and A. Seilacher, pp. 293-309, Springer, New York, 1997.

Gomberg, J., and S. Davis, Stress/strain changes and triggered seismicity at the Geysers, California, *J. Geophys. Res., 101,* 733-749, 1996.

Hill, D. P., et al., Seismicity remotely triggered by the magnitude 7.3 Landers, California, earthquake, *Science, 260,* 1617-1623, 1993.

Kanamori, H., and D. L. Anderson, Theoretical basis of some empirical relations in seismology, *Bull. Seismol. Soc. Am., 65,* 1073-1095, 1975.

Lockner, D. A., and N. M. Beeler, Premonitory slip and tidal triggering of earthquakes, *J. Geophys. Res., 104,* 20,133-20,151, 1999.

Melchior, P., *The tides of the planet Earth,* 641 pp., Pergamon, New York, 1983.

Mofjeld, H. O., F. I. Gonzles, M. C. Eble, and J. C. Newman, Ocean tides in the continental margin of the Pacific Northwest shelf, *J. Geophys. Res., 100,* 10,789-10,800, 1995.

Reasenberg, P., Second-order moment of central California seismicity, 1969-1982, *J. Geophys. Res., 90,* 5479-5495, 1985.

Rydelek, P. A., I. S. Sacks, and R. Scarpa, On tidal triggering of earthquakes at Campi Flegrei, Italy, *Geophys. J. Int, 109,* 125-137, 1992.

Schwiderski, E. W., On charting global ocean tides, *Rev. Geophys. Space Phys., 18,* 243-268, 1980.

Tolstoy, M., F. L. Vernon, J. A. Orcutt, and F. K. Wyatt, The breathing of the seafloor: Tidal correlations of seismicity at Axial volcano, *Geology,* submitted, 2001.

Tsuruoka, H., M. Ohtake, and H. Sato, Statistical test of the tidal triggering of earthquakes: Contribution of the ocean tide loading effect, *Geophys. J. Int., 122,* 183-194, 1995.

Vidale, J. E., D. C. Agnew, M. J. S. Johnston, and D. H. Oppenheimer, Absence of earthquake correlation with Earth tides: An indication of high preseismic fault stress rate, *J. Geophys. Res., 103,* 24,567-24,572, 1998.

Wilcock, W. S. D., S. D. Archer, and G. M. Purdy, Microearthquakes on the Endeavour segment of the Juan de Fuca Ridge, *J. Geophys. Res.,* submitted, 2001.

W. S. D. Wilcock, School of Oceanography, University of Washington, Box 357940, Seattle, WA 98195. (e-mail: wilcock@ocean.washington.edu)

(Received May 1, 2001; revised July 6, 2001;
accepted August 2, 2001.)